# Phase stability of the intermetallic $L2_1$ Heusler alloys of $A_2(Hf_{1-x}Zr_x)Al$ (where $A$=Pd and Pt) for an Nb-based high-temperature materials design

Miyoung Kim
*Department of Physics and Astronomy, Northwestern University, Evanston, Illinois 60208, and BK21 Physics Research Division, Seoul National University, Seoul, Korea*

A. J. Freeman[a)]
*Department of Physics and Astronomy, Northwestern University, Evanston, Illinois 60208*

Sungtae Kim and J. H. Perepezko
*Department of Materials Science and Engineering, University of Wisconsin, Madison, Wisconsin 53706*

G. B. Olson
*Department of Materials Science and Engineering, Northwestern University, Evanston, Illinois 60208*

(Received 13 June 2005; accepted 27 September 2005; published online 21 December 2005)

First principles phase stability calculations are used to predict the lattice mismatches between Nb and the $A_2(Hf_{1-x}Zr_x)Al$ $L2_1$ Heusler phases and the $L2_1$ phase formation energies, where $A$=Pd and/or Pt, and $x$=0, 0.25, 0.75 and 1. The calculated $L2_1$ phase mixing energy demonstrates that the Hf-Zr solution phases in the form of $A_2(Hf_{1-x}Zr_x)Al$ ($x \neq 0$ and 1) are energetically favored, although the Zr-rich alloys exhibit a smaller lattice mismatch than the Hf-rich alloys. The introduction of Pt reduces the lattice mismatch, and forms the energetically favorable (PtPd)XAl Heusler phase, where $X$=Hf and Zr. A number of critical diffusion couple experiments confirm the phase stability predictions and establish new microstructural design parameters. © *2005 American Institute of Physics*. [DOI: 10.1063/1.2136223]

The design of materials for high-temperature operation is a critical challenge for aerospace applications that requires the concurrent attainment of a high melting point, good oxidation resistance, and low density, together with high-temperature strength and adequate ductility. While the Ni-base superalloys are in current widespread use, their melting temperature limits further improvement of their high-temperature capabilities. While a modest increase in high-temperature capability is possible with NiAl-(B2-) based alloys, Nb, and Nb based alloys are more attractive candidates because of the high melting temperature (2468 °C), low density ($(8.6\times10^3$ kg/m$^3$) and lower diffusivity of Nb compared to that of Ni. In designing Nb-based high-temperature materials, it is quite appealing to search for the $L2_1$ ternary compounds that can be combined with Nb—in analogy with the NiAl-based alloys; there, the effective way of overcoming its low ductility and loss of strength at high temperatures was found with the inclusion of ternary elements such as the $L2_1$ phase $Ni_2XAl$ compounds, where $X$ are group IVA and VA elements.[1]

The $Ni_2XAl$ alloys have a large lattice mismatch with Nb (−8–11%),[2] which makes their combination with Nb as a multiphase design unfavorable. Instead, the $Pd_2XAl$ Heusler phases have been identified as good candidates since their lattice mismatch with Nb is much smaller (−3.05% and −3.55% for $X$=Zr and Hf, respectively) than those of the $Ni_2XAl$ alloys,[3,4] and thermodynamic compatibility of $Pd_2HfAl$ in Nb at a desired use tumperature of 1300° C has been demonstrated.[3] Furthermore, the group VIII element Pt has a larger size than Pd so that it is expected that the $Pt_2XAl$ phase exhibits a larger lattice parameter compared to the $Pd_2XAl$ phase. Since the lattice mismatch is a key parameter for the design of multiphase high-temperature alloys, the inclusion of $Pt_2XAl$ type metastable Heusler phases into a Nb-based alloy design is an effective strategy to get a further reduction of the Nb lattice mismatch.

Now, since the stable $Pt_2HfAl$ phase exists in a hexagonal $AsNa_3$ structure, it is necessary to evaluate the phase stability for the Heusler $L2_1$-based alloys $A_2(Hf_{1-x}Zr_x)Al$, where $A$=Pd and/or Pt, by performing highly precise first principles electronic structure calculations using the full-potential linearized augmented plane wave (FLAPW)[5] method. The energy calculations are undertaken as part of a broader research effort in which entropic contributions to the alloy thermodynamics are deduced from measured high-temperature phase relations.[4] In this paper, the possibility of obtaining Hf–Zr solution phase formation is examined by comparing the formation energy of the *separate single phases* ($x$=0 or 1) with that of the *solution phases* ($x$=0.25 or 0.75). In addition, the Pt–Pd solution phases of the PtPdHfAl and PtPdZrAl alloys are also calculated. The results obtained predict the possible interdiffusive mixing of Hf and Zr between the existing separate single phases of $A_2HfAl$ and $A_2ZrAl$ for both $A$=Pd and Pt, with the mixing energy of −0.1–−0.9 mRy/f.u. depending on the composition ratio of Hf and Zr. A complete mixing was confirmed by EPMA measurements and SEM observations on a diffusion couple for the Pd case. Also, the Pt–Pd solution $L2_1$ phase in the form of $PtPdXAl$ is shown to be energetically favored over the separate single phases of $Pt_2XAl$ and $Pd_2XAl$ for both $X$=Hf and Zr with their mixing energies one order larger compared to the Hf-Zr mixing phases. As a promising candidate-strengthening phase for Nb-based high-temperature alloys, the inclusion of Zr and Pt in the $L2_1$

[a)]Author to whom correspondence should be addressed.

 

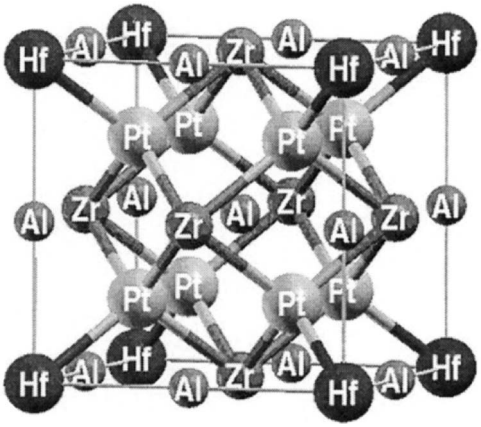


FIG. 1. Atomic structures of the mixed phase, $Pt_2(Hf_{0.75}Zr_{0.25})Al$. Note that the replacement of Hf with Zr generates the $L2_1$ Heusler alloy of $Pt_2ZrAl$.

Heusler-type phases indicates an advantage of a reduced lattice mismatch with a Nb matrix.

The atomic structure of the *single phase* has four atoms in a primitive unit cell. Then, the *solution phase* of Hf and Zr, $A_2(Hf_{1-x}Zr_x)Al$, is formed by stacking these cubic cells of $A_2HfAl$ and $A_2ZrAl$ into a $2\times2\times2$ structure, so that the Hf and Zr atoms form the $L1_2$ cubic structure, where the primitive unit cell has 16 atoms [cf. Fig. 1 for $Pt_2(Hf_{0.25}Zr_{0.75})Al$]. The lattice constants are determined from total energy calculations within both the local density approximation (LDA)[6] and the generalized gradient approximation (GGA).[7] The formation energy, $E_{form}$, is calculated by subtracting the sum of the total energies for the constituent metals from the total energy of the compound, that is, $E_{form}=E(M_aN_b)-[aE(M)+bE(N)]$.

The calculated lattice constants, lattice mismatch with Nb, and formation energies are listed in Table I. For the lattice constants, the local density approximation (LDA) predicts good agreement with the experiment (to within a 0.1% and 0.2% mismatch) while the generalized gradient approximation (GGA) overestimates them by 1.2% and 1.4% for $Pd_2HfAl$ and $Pd_2ZrAl$, respectively. Thus, the LDA provides reliable lattice constants for these materials, even though GGA is known to give good bond lengths for some $3d$-transition metal compounds, and so further discussion will be based on the LDA results.

As expected, the Pt Heusler alloys give larger lattice constants than those for the Pd alloys. In terms of the lattice misfit with Nb, choosing Zr as the quaternary element is found to be more favorable over the Hf or the solution phase of Hf and Zr, among which the single phase of $Pt_2ZrAl$ is best with a $-2.60\%$ of misfit. However, the calculation predicts that the Hf alloys show larger formation energies compared to the Zr alloys (cf. $Pd_2HfAl$ vs $Pd_2ZrAl$ or $Pt_2HfAl$ vs $Pt_2ZrAl$). Consistent with this, the solution phase with more Hf [i.e., $A_2(Hf_{0.75}Zr_{0.25})Al$] has a larger formation energy than those with more Zr [i.e., $A_2(Hf_{0.25}Zr_{0.75})Al$].

Another interesting, and probably more important, result is that the solution phases are energetically favored over the separate single phases. A formation energy comparison of the alloys with $x=0.25$ or 0.75 (solution phase) with those with $x=0$ or 1 (separate single phases) shows that there will be a slight energy gain of the Hf-Zr solution phase formation over the separate single phases. In order to demonstrate the phase stability clearly, the calculated mixing energy, $E_{mixing}$, is shown in Table I. The mixing energy is defined by the formation energy difference of the solution and separate phases. A negative mixing energy means that the solution phase is energetically more stable over the separate single phases. For example, the formation energy of the solution phase $Pt_2(Hf_{0.75}Zr_{0.25})Al$ from $Pt_2HfAl$ and $Pt_2ZrAl$ is calculated by

$$\begin{aligned}E_{mixing}[Pt_2(Hf_{0.75}Zr_{0.25})Al] &= 1/4\{E_{form}[Pt_2(Hf_{0.75}Zr_{0.25})Al] \\ &\quad -[3E_{form}(Pt_2HfAl)+E_{form}(Pt_2ZrAl)]\} \\ &= -0.7\ \text{mRy},\end{aligned}$$

meaning that the formation $Pt_2(Hf_{0.75}Zr_{0.25})Al$ from $Pt_2HfAl$ and $Pt_2ZrAl$ will release 0.7 mRy per four-atoms-formula unit. As can be seen from Table I, it was found that all solution phases (the solution of Hf-Zr as well as Pt-Pd) are energetically preferred over the separate single phases, with the mixing energy of Pt-Pd larger by one order compared to the Hf-Zr mixing case.

The predicted phase stability of the Hf-Zr solution phase, $Pd_2(Hf,Zr)Al$, was examined critically by performing a $Pd_2HfAl/Pd_2ZrAl$ diffusion couple experiment. The $Pd_2HfAl$ and $Pd_2ZrAl$ alloys were initially prepared by re-

TABLE I. The calculated lattice constants, the lattice mismatch with Nb, the formation energy, and the mixing energy. For easy comparison, the energies are given in mRy per four-atoms formula unit (f.u.). The error bar is ±0.05 mRy/f.u. for the calculated energies.

| | Lattice constant (nm) | | | Nb mismatch (%) | $E_{form}$ (mRy/f.u.) | $E_{mixing}$ (mRy/f.u.) |
|---|---|---|---|---|---|---|
| | LDA | GGA | Exp. | LDA | LDA | LDA |
| $Pd_2HfAl$ | 0.635 | 0.646 | 0.637 | −3.8 | 243.6 | |
| $Pd_2ZrAl$ | 0.639 | 0.647 | 0.640 | −3.2 | 242.4 | |
| $Pd_2(Hf_{0.75}Zr_{0.25})Al$ | 0.634 | 0.646 | | −4.0 | 243.6 | −0.3 |
| $Pd_2(Hf_{0.25}Zr_{0.75})Al$ | 0.636 | 0.647 | | −3.7 | 242.9 | −0.9 |
| $Pt_2HfAl$ | 0.642 | 0.650 | | −2.8 | 287.4 | |
| $Pt_2ZrAl$ | 0.643 | 0.651 | | −2.6 | 284.2 | |
| $Pt_2(Hf_{0.75}Zr_{0.25})Al$ | 0.638 | 0.649 | | −3.4 | 287.3 | −0.7 |
| $Pt_2(Hf_{0.25}Zr_{0.75})Al$ | 0.641 | 0.650 | | −2.9 | 285.1 | −0.1 |
| PtPdHfAl | 0.636 | 0.648 | | −3.7 | 276.2 | −10.7 |
| PtPdZrAl | 0.640 | 0.648 | | −3.1 | 272.8 | −9.5 |

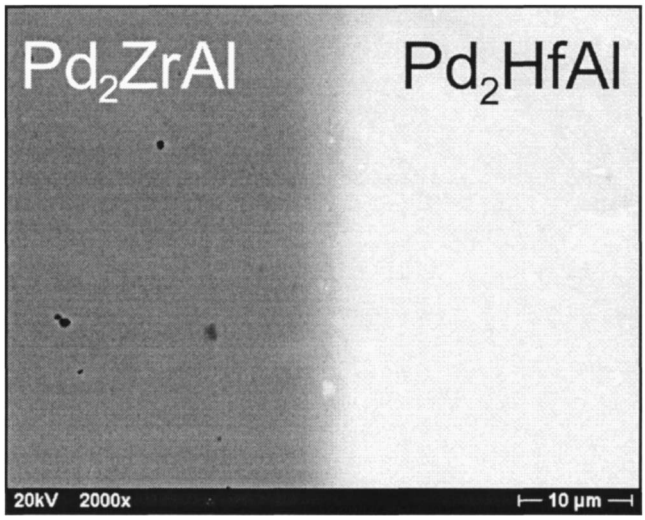


FIG. 2. BSE image of a cross section of the $Pd_2HfAl/Pd_2ZrAl$ diffusion couple annealed at 1100 °C for 50 h.

peated arc melting of pure Pd, Al, Hf, and Zr metals under a Ti-gettered pure argon (99.998%) atmosphere. A differential thermal analysis (DTA) examination indicated that as-cast $Pd_2HfAl$ and $Pd_2ZrAl$ alloys begin melting at ~1440 °C and ~1350 °C, respectively. The $Pd_2HfAl$ and $Pd_2ZrAl$ alloys wrapped with pure Ta foils were homogenized at 1200 °C for 100 h under a Ti-gettered argon atmosphere and followed by furnace cooling. The $Pd_2HfAl$ and $Pd_2ZrAl$ alloys were then sliced and assembled into a diffusion couple. To test for the intermixing of Hf and Zr at high temperature, the $Pd_2HfAl/Pd_2ZrAl$ diffusion couple was annealed at 1100 °C for 50 h. A backscattered electron (BSE) image of the cross section of the $Pd_2HfAl/Pd_2ZrAl$ diffusion couple is shown in Fig. 2, where a continuously varying contrast was observed in the diffusion reaction zone between $Pd_2HfAl$ and $Pd_2ZrAl$.

Focusing on the case with the weaker mixing interaction, for further analysis, an electron probe microanalysis (EPMA) was used to measure the Pd, Hf, Zr, and Al concentrations (Fig. 3) over the diffusion reaction zone. The EPMA analysis was carried out on the uncoated specimens at an acceleration voltage of 18 kV and a beam current of 20 nA, which eliminated Zr K$\alpha$ excitation and interference with Hf L$\alpha$. A "Probe for Window" software[8] solved serious interference problems of the sixth-order Hf L$\beta$4 and second-order Pd L$\beta$1 lines with the first-order Al K$\alpha$ line, and the first order Hf M5-O1 line with the first-order Zr L$\alpha$ line. In reality, it is difficult to synthesize an alloy with a composition in exact coincidence with the nominal composition. Thus, compositions of both $Pd_2HfAl$ and $Pd_2ZrAl$ can deviate from their exact stoichiometric compositions and retain the phase structure, meaning that the Pd and Al concentrations in the $Pd_2HfAl$ and $Pd_2ZrAl$ phases need not be exactly the same. Most importantly, Fig. 3 exhibits the symmetrical change of

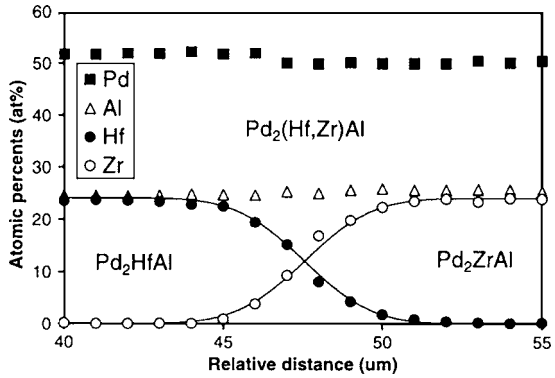


FIG. 3. Concentration profiles obtained from the diffusion couple shown in Fig. 2 by EPMA.

the Hf and Zr concentrations over the diffusion reaction zone, indicating that their composition sum is constant. In other words, the Hf and Zr atoms substitute readily for each other and form a complete solid solution of $Pd_2(Hf_{1-x}Zr_x)Al$ over the entire diffusion reaction zone, in full agreement with the calculation prediction. A more detailed phase diagram study is highly desirable to provide further essential information on the phase and microstructure development of Nb-$L2_1$ combinations.

This example supports the reliability of integrating rigorous first-principles calculations in the thermodynamic design of complex multicomponent alloys.[4] Specific parameters determined here provide important input for quantitative optimization of the multicomponent (Pd,Pt)2(Hf,Zr)AlL21 phase, balancing a tradeoff among thermodynamic stability, lattice misfit, and raw material cost in the pursuit of Nb-based superalloys capable of operation at 1300 °C.

The financial support of AFOSR MEANS Grant No. F49620-01-1-0529 is gratefully acknowledged.

[1] Y. Koizmi, Mater. Sci. Eng., A, **233**, 36 (1997); Y. Umakoshi, M. Yamaguchi, and T. Yamane, Philos. Mag. A **52**, 357 (1985); P. R. Strutt, R. S. Polvani, and J. C. Ingram, Metall. Trans. A **7**, 23 (1976); K. Vedula, V. Pathare, I. Aslanidis, and R. H. Titran, in *High-Temperature Ordered Intermetallic Alloys III*, p. 411; M. Takeyama and C. T. Liu, J. Mater. Res. **5**, 1189 (1990).
[2] W. Lin and A. J. Freeman, Phys. Rev. B **45**, 61 (1992).
[3] A. Misra, R. Bishop, G. Ghosh, and G. B. Olson, Metall. Mater. Trans. A **34A**, 1771 (2003).
[4] G. B. Olson, A. J. Freeman, P. W. Voorhees, G. Ghosh, J. Perepezko, M. Eberhart, and C. Woodward, in *Intl. Symp. Niobium for High Temperature Applications*, edited by Y.-W. Kim, and T. Carneiro (The Minerals, Metals and Materials Society, Warrendale, PA, 2004), p. 113.
[5] E. Wimmer, H. Krakauer, M. Weinert, and A. J. Freeman, Phys. Rev. B **24** 864 (1981), and references therein.
[6] L. Hedin and B. I. Lundqvist, J. Phys. C **4**, 2064 (1971).
[7] J. P. Perdew, K. Burke, and M. Ernzerhof, Phys. Rev. Lett. **77**, 3865 (1996).
[8] J. H. Fournelle, J. J. Donovan, S. Kim, and J. H. Perepezko, *Proceedings of 2nd Conference of the International Union of Microbeam Analysis Societies*, 2000, p. 425.